SAND2018-9845C

A comparison of mesh-free and mesh-based Lagrangian approximations of manufactured shear-dominated deformation fields

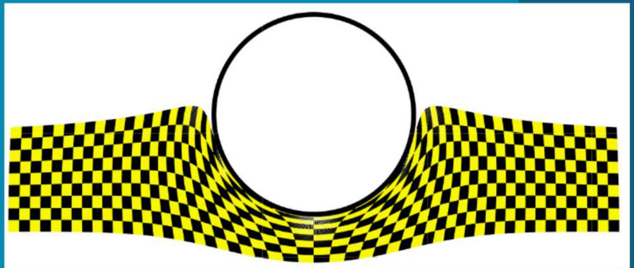

Joe Bishop

Engineering Sciences Center
Sandia National Laboratories
Albuquerque, NM

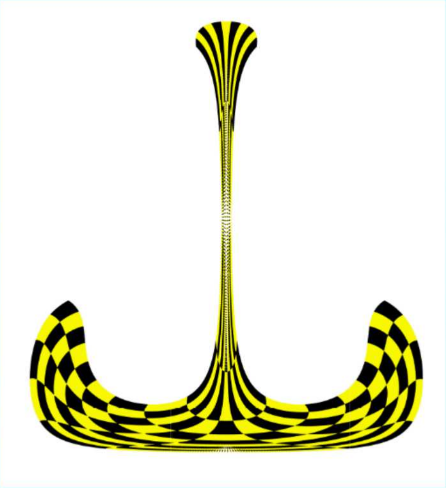

USACM Thematic Conference on Meshfree and Particle Methods,
September 10-12, 2018, Santa Fe, NM.

Outline

1. Value proposition for meshfree
2. Modeling challenges for meshfree
3. Examples of limitations of mesh-based discretizations for extreme events
4. Verification example for exploring robustness of FE vs meshfree discretizations
5. Summary

Value proposition for meshfree

- ease of discretization
  - use of point cloud and surface representation
- robust large deformation
  - shape functions defined on reference configuration
- local adaptivity
  - hp adaptivity – easy to change approximation order
- conversion from Lagrangian to semi-Lagrangian
  - "seamless" update of connectivity without tangling

(robust large deformation; shape functions defined on reference configuration) } focus of this talk

Modeling challenges for meshfree

- surface representation
  - explicit vs. implicit representation
  - adaptivity on surface
  - new surface generation for fracture
- nonconvex domains
  - weight functions around re-entrant corners
- assemblies of parts, material interfaces
- consistent quadrature, stabilization
  - stress points vs. nodal integration
  - integration consistency

Large deformation example

EFP formation process with copper liner

(Liu, et.al, 2017, International Journal of Impact Engineering, 109, 264-275)

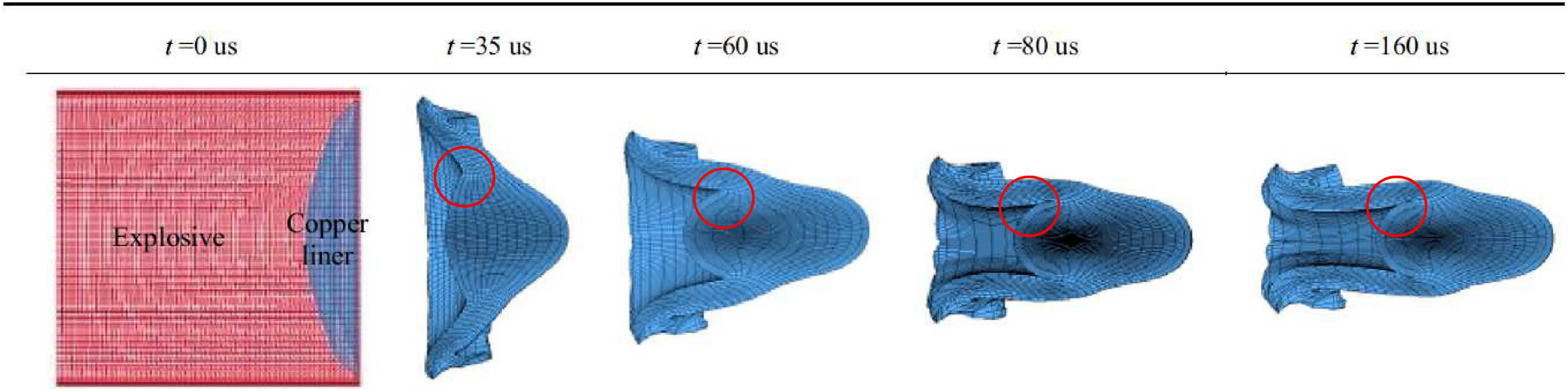

Shear localization

SANDIA REPORT

SAND2015-2850
Unlimited Release
Printed April, 2015

An Experimental Study of Shear-Dominated Failure in the 2013 Sandia Fracture Challenge Specimen

Edmundo Corona, Lisa A. Deibler, Benjamin Reedlunn, Mathew D. Ingraham and Shelley Williams

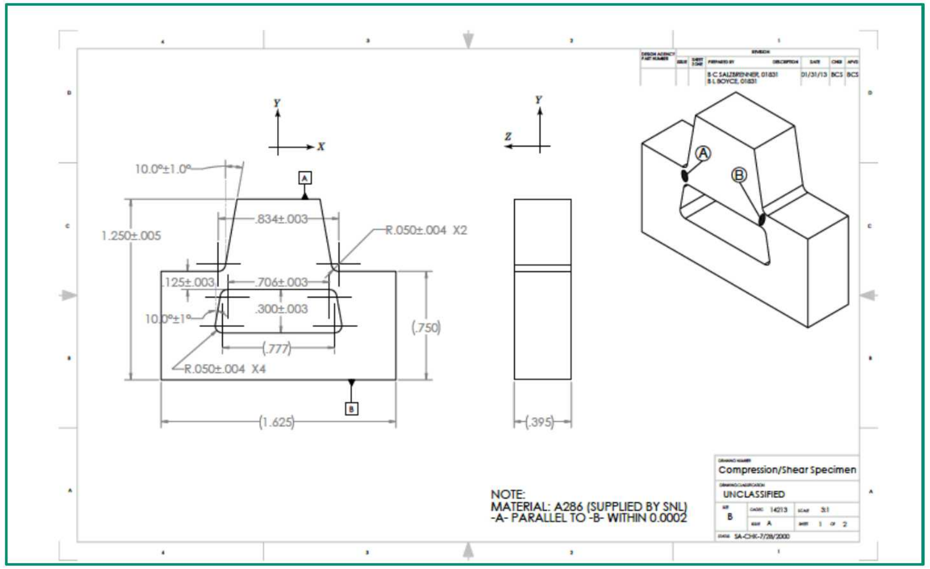

- A286 steel
- 7075 aluminum

Shear localization

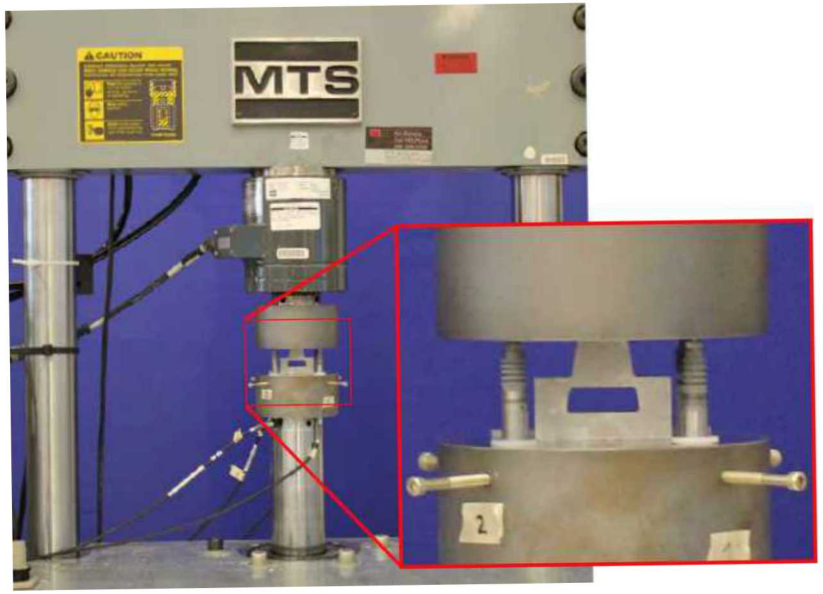

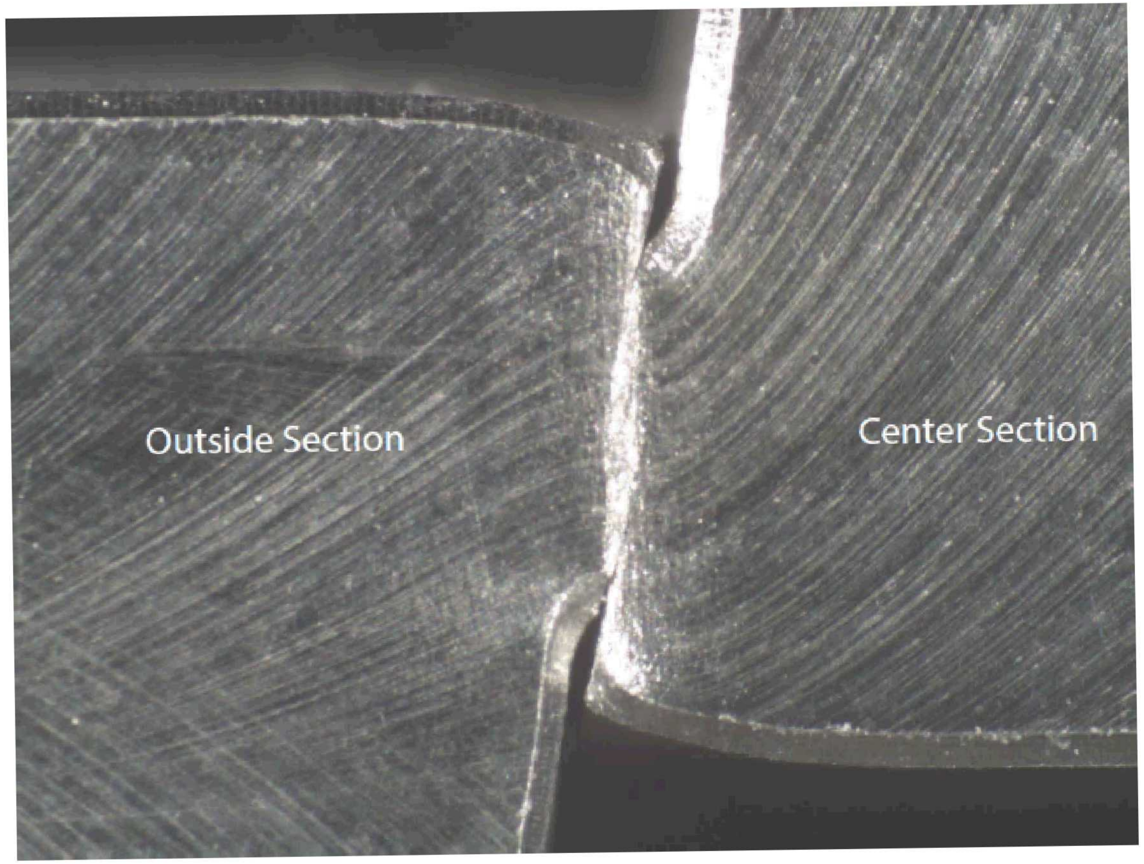

Sierra/RKPM (Jake Koester, Frank Beckwith)

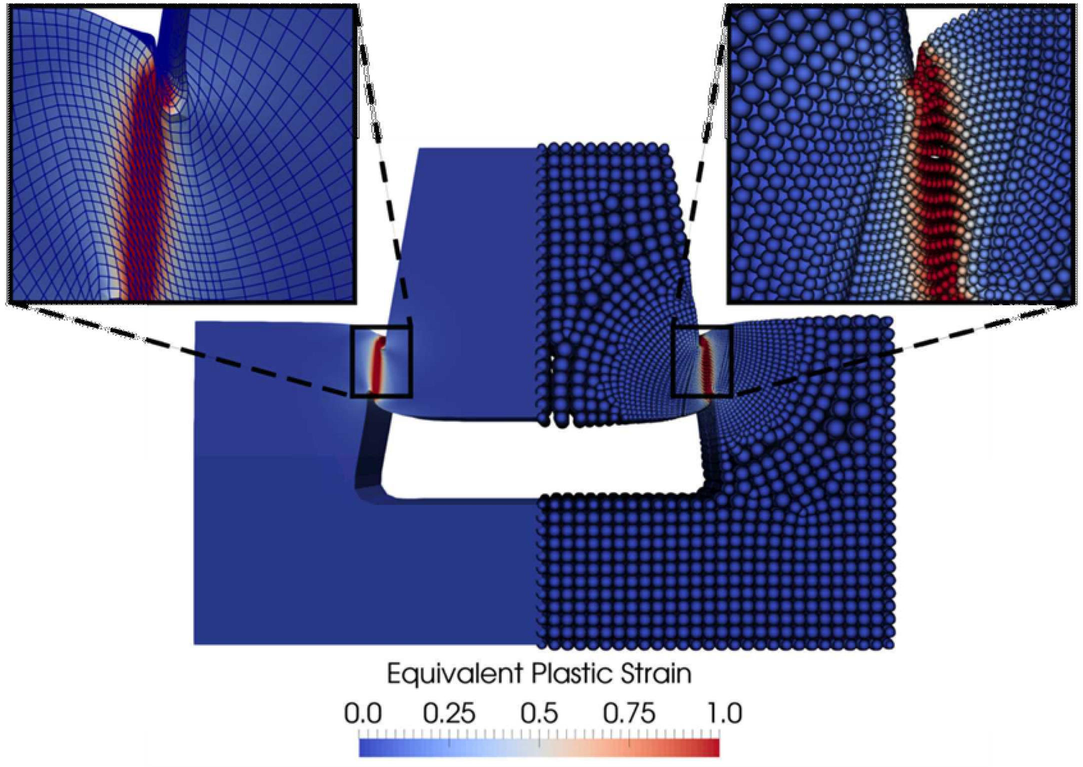

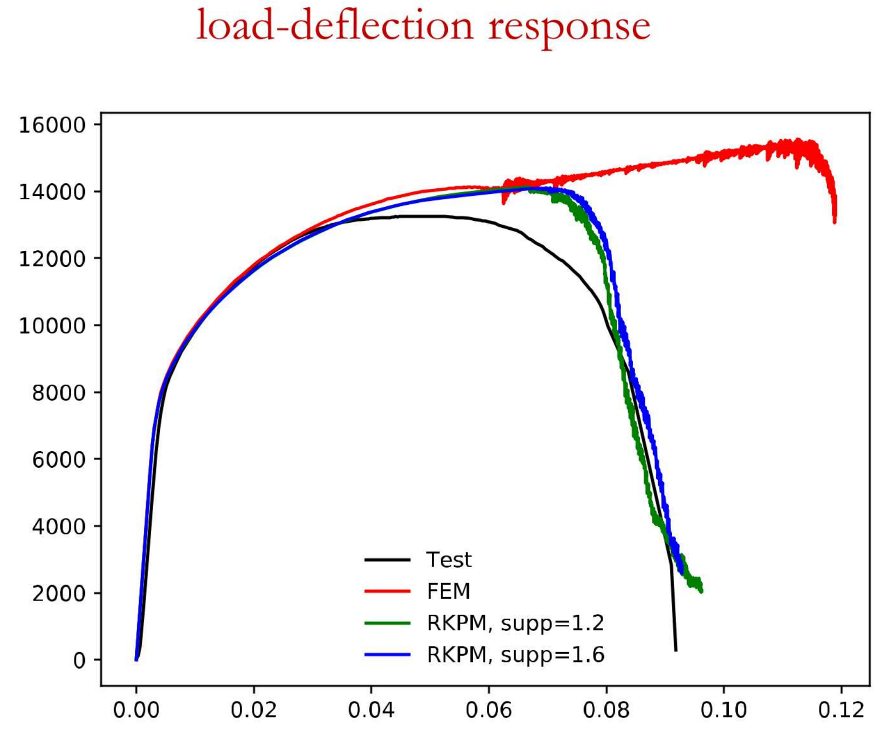

ALEGRA / SHISM (Soft-Hard Interface Surface Mechanics)

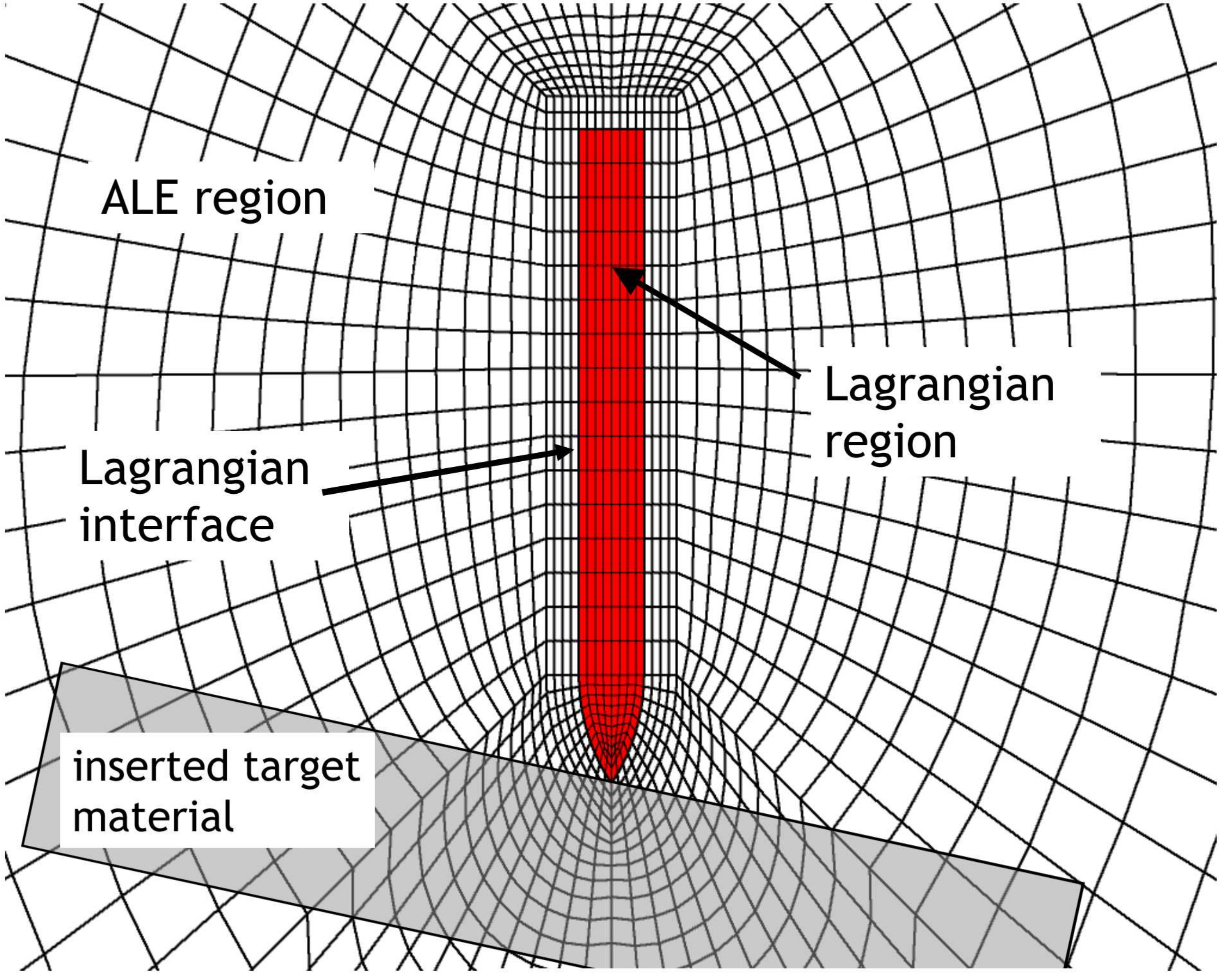

- External ALE mesh 'tracks' the c.m. of the penetrator (translation and rotation).
- Target material 'flows' around the penetrator.
- External mesh interacts with penetrator via contact algorithm.

Assumptions

1. The penetrator is much harder than the target.
2. The target material may flow extensively around the penetrator.
3. There is no penetrator erosion or breakup, but the penetrator may exhibit significant deformation.

Bishop and Voth, "Semi-Infinite Target Penetration by Ogive-Nose Penetrators: ALEGRA/SHISM Code Predictions for Ideal and Nonideal Impacts," JPVT, 2009. **131**

Effect of AOA at high striking velocities

Bishop and Voth, “Semi-Infinite Target Penetration by Ogive-Nose Penetrators: ALEGRA/SHISM Code Predictions for Ideal and Nonideal Impacts,” JPVT, 2009. **131**

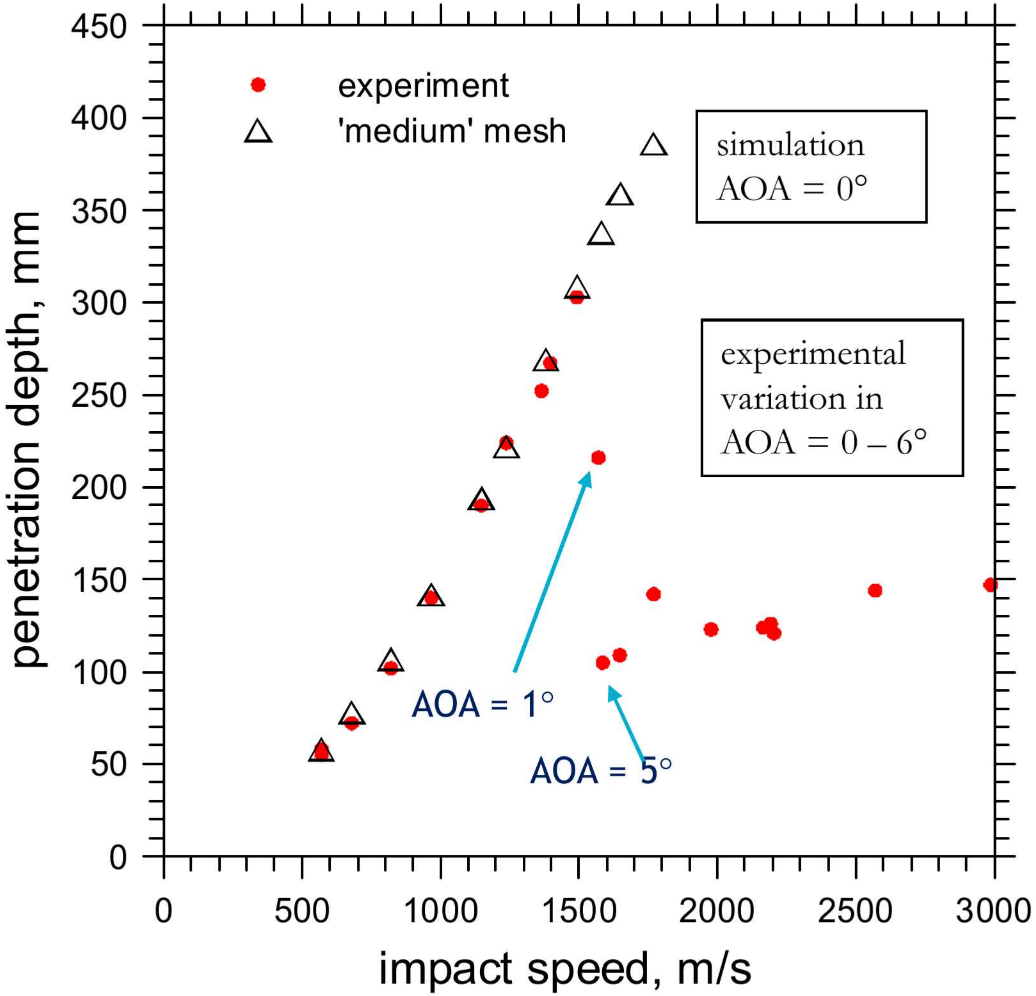

Modest changes in AOA can have catastrophic effects on penetrator deformation.

V_s=1580 m/s, AOA=0°

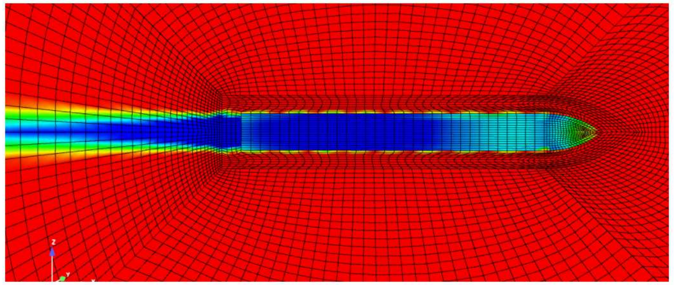

V_s=1580 m/s, AOA=2°

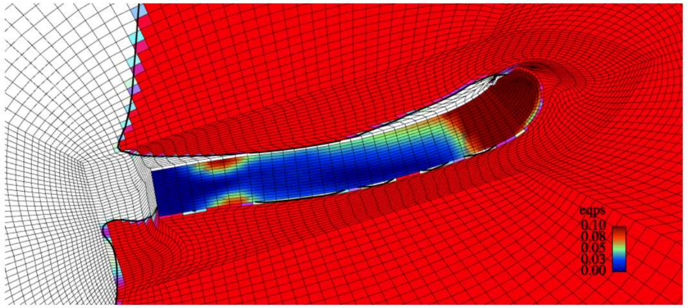

Normal Impact, V_s = 1580 m/s, AOA = 2°

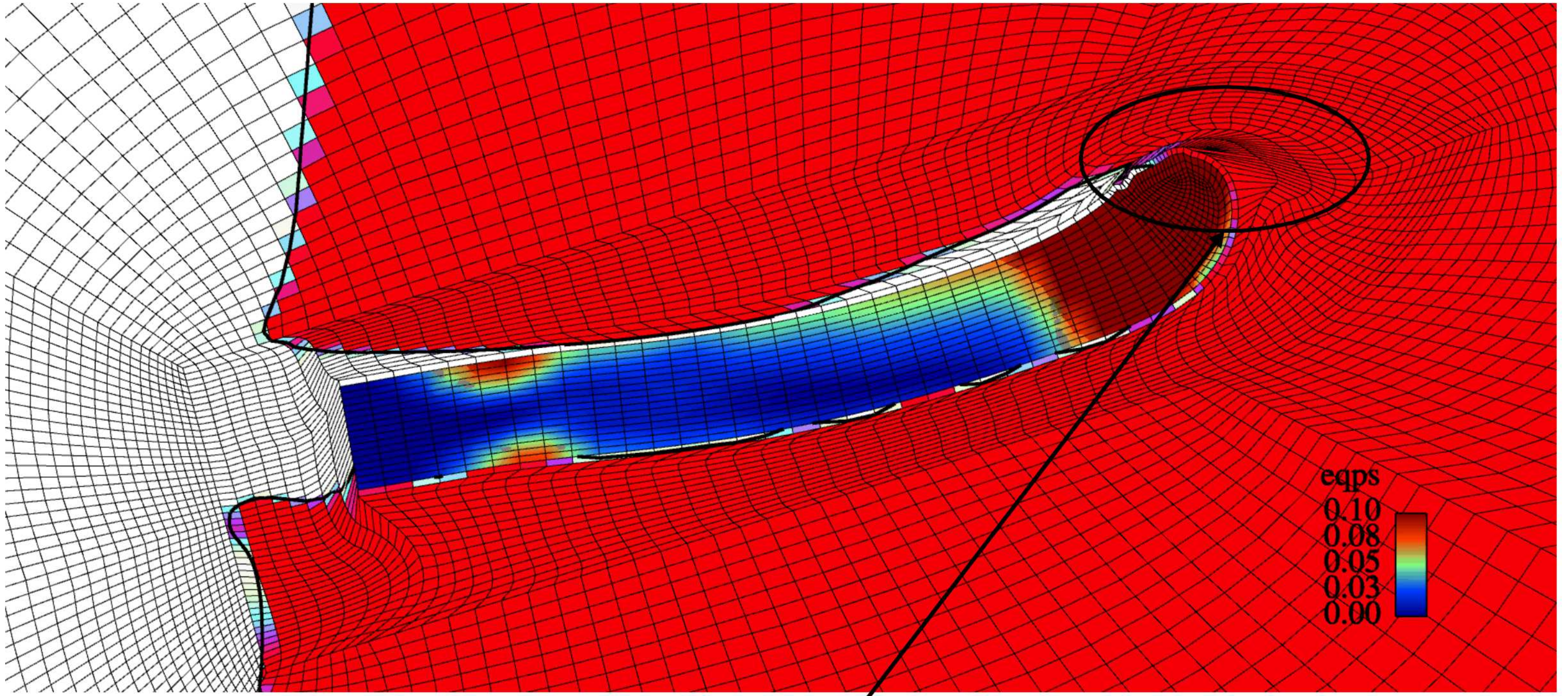

severe mesh distortion at t = 50 μs prevents further simulation

Bishop and Voth, "Semi-Infinite Target Penetration by Ogive-Nose Penetrators: ALEGRA/SHISM Code Predictions for Ideal and Nonideal Impacts," JPVT, 2009. **131**

Comparison of mesh-free and mesh-based Lagrangian approximations of a manufactured shear-dominated deformation field

- Would like to develop an exact solution to compare FE to meshfree discretizations.
- Use to compare robustness, sensitivity to initial distortion.
- Use to explore surface representations.
- Use to explore adaptivity.

- In this talk, explore best-approximation error, FE vs. MLS

Interpolation bounds for isoparametric finite element spaces

for linear elements (shape regular)

$$||u - I^h u||_0 \leq c\, h^2\, |u|_2$$

interpolation operator

L[2] norm

$$||u - I^h u||_1 \leq c\, h\, |u|_2$$

H[1] norm

similar bounds for MLS space

Best approximation

best approximation in H^1 $\hat{u} = \arg\min_{u \in V^h} ||u - u^{\text{exact}}||_{H^1}$

so $||\hat{u} - u^{\text{exact}}||_{H^1} \leq ||I^h u^{\text{exact}} - u^{\text{exact}}||_{H^1}$

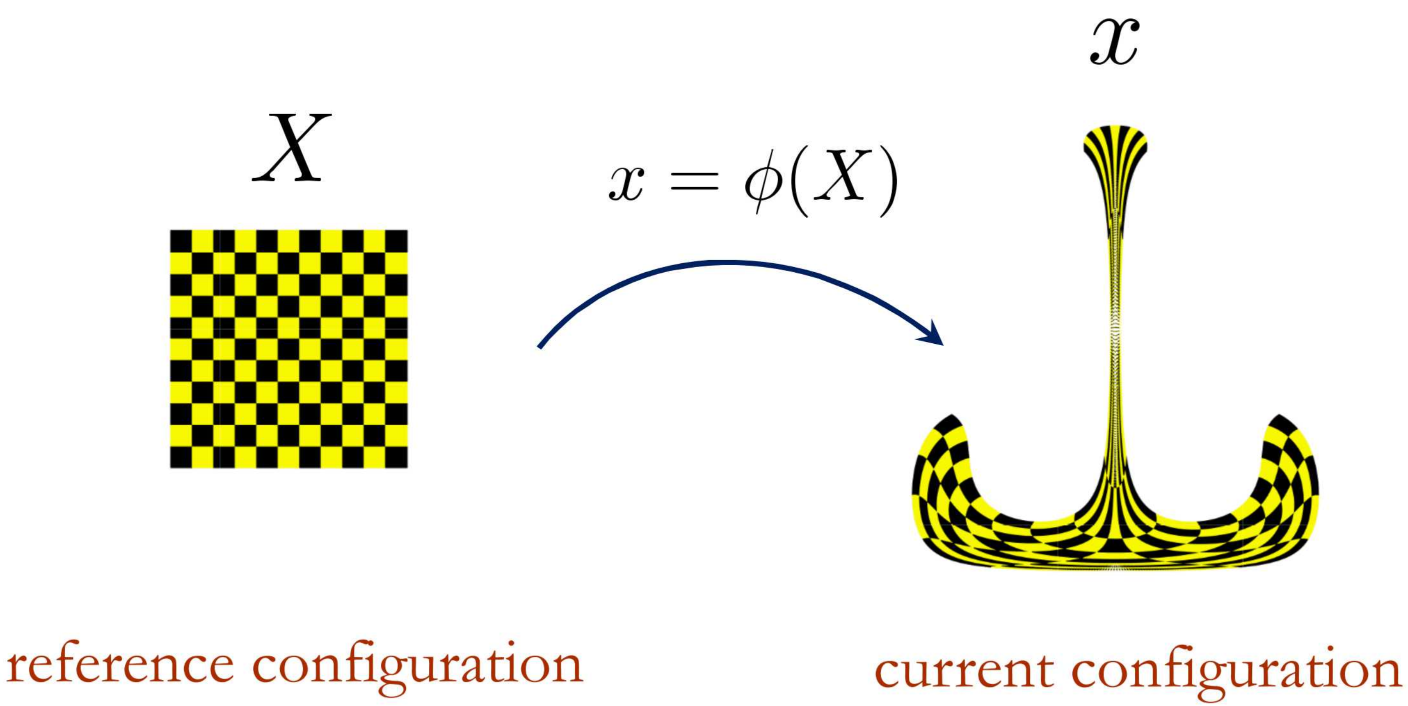
X
x
x = φ(X)
reference configuration
current configuration

Define deformation map using stream function

$$\Psi = \frac{1}{4\pi} \sin[4\pi(x_1 + 1/2)] \cos[4\pi(x_2 + 1/2)]$$

$$v_1 = -\frac{\partial \Psi}{\partial x_2} , \quad v_2 = \frac{\partial \Psi}{\partial x_1}$$

divergence free since $$\nabla \cdot v = \frac{\partial v_1}{\partial x_1} + \frac{\partial v_2}{\partial x_2} = -\frac{\partial^2 \Psi}{\partial x_1 \partial x_2} + \frac{\partial^2 \Psi}{\partial x_2 \partial x_1} = 0$$

isochoric $J = \det(F) = 1$ for all time F is deformation gradient

How to convert this Eulerian description to Lagrangian?

$t = 0$

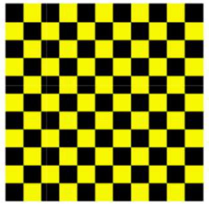

$t = 0.125$

$t = 0.25$

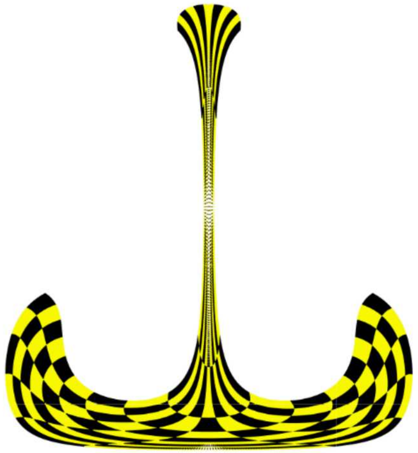

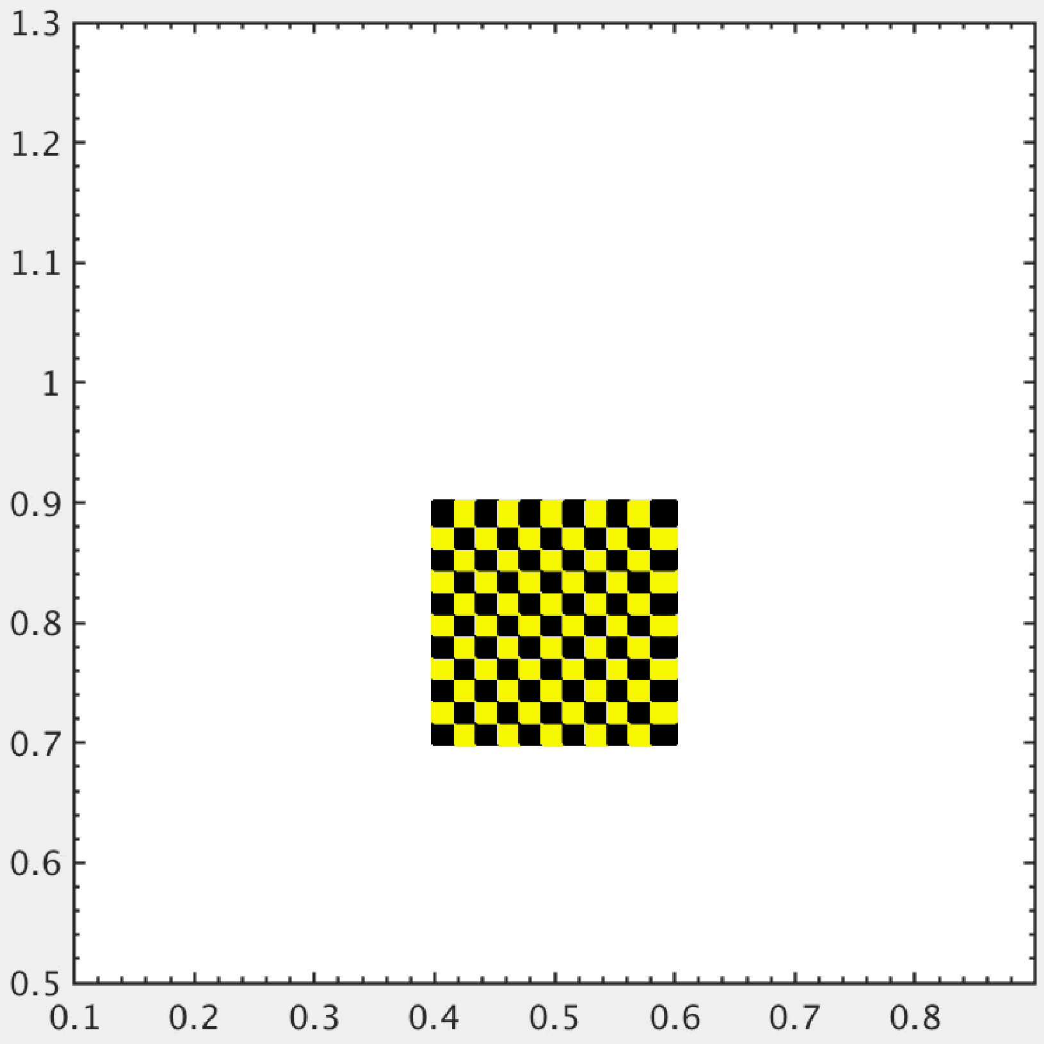
1.3
1.2
1.1
1
0.9
0.8
0.7
0.6
0.5
0.1
0.2
0.3
0.4
0.5
0.6
0.7
0.8

$$\Psi = r \sin\theta \left(1 - \frac{1}{r^2}\right) \qquad r^2 = x_1^2 + x_2^2$$

$$\tan\theta = x_2/x_1$$

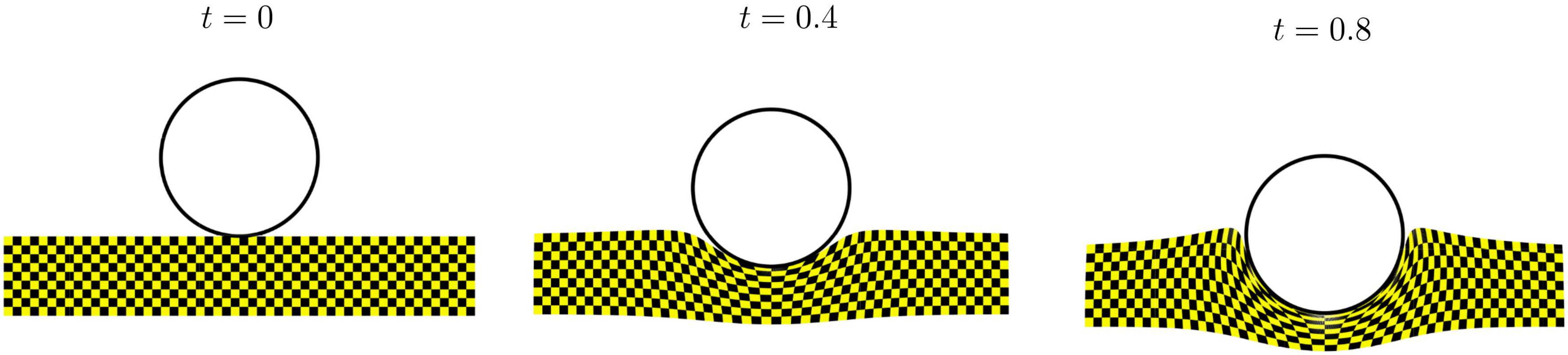

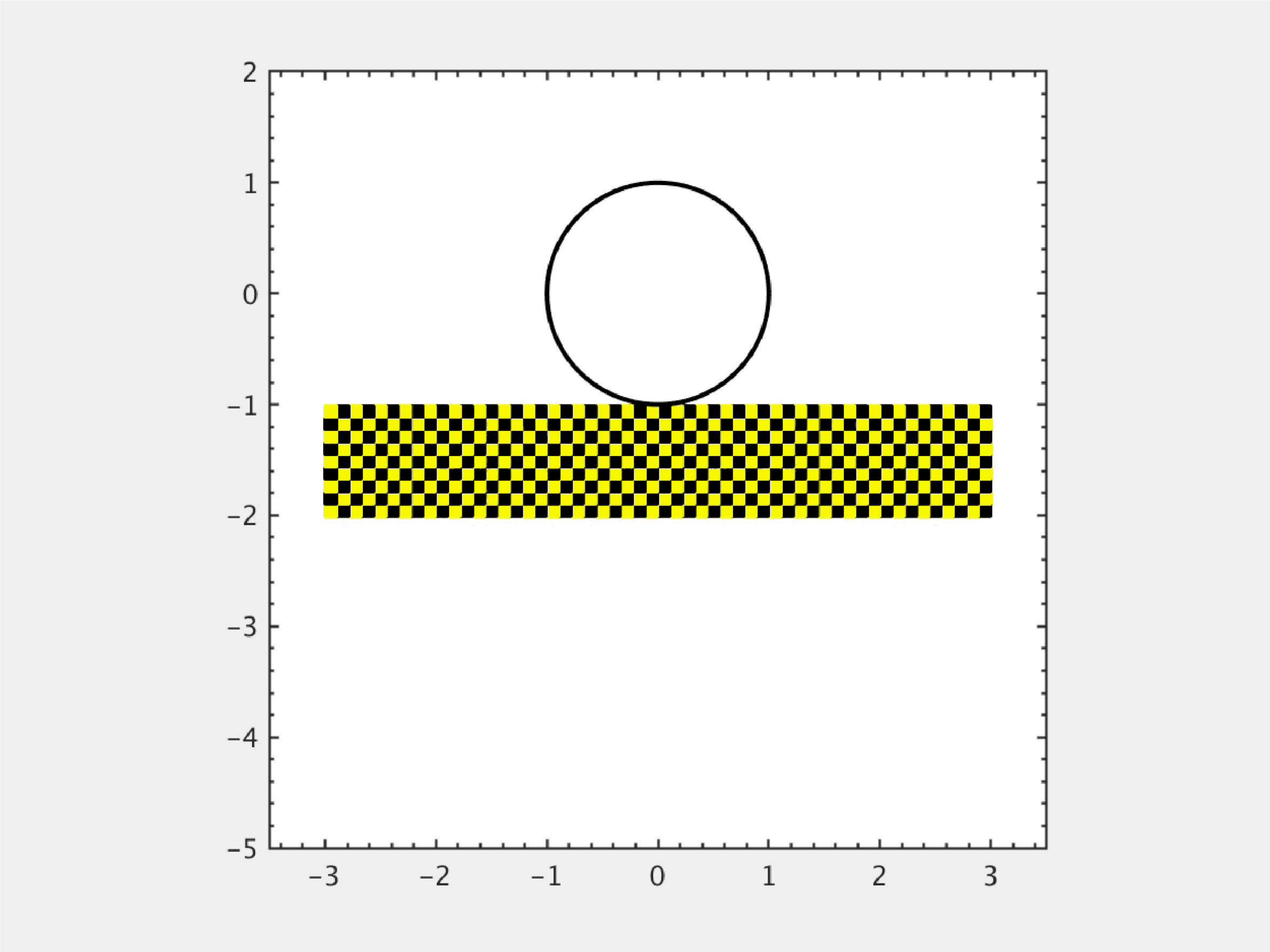
2
1
0
−1
−2
−3
−4
−5
−3
−2
−1
0
1
2
3

How to convert Eulerian description to Lagrangian?

$$\dot{F} = \frac{\partial v}{\partial X} = \frac{\partial v}{\partial x}\frac{\partial x}{\partial X} = lF$$

l is velocity gradient

$$l = \begin{bmatrix} l_{11} & l_{12} \\ l_{21} & l_{22} \end{bmatrix} = \begin{bmatrix} \partial v_1/\partial x_1 & \partial v_1/\partial x_2 \\ \partial v_2/\partial x_1 & \partial v_2/\partial x_2 \end{bmatrix}$$

$$F = \begin{bmatrix} F_{11} & F_{12} \\ F_{21} & F_{22} \end{bmatrix} = \begin{bmatrix} \partial x_1/\partial X_1 & \partial x_1/\partial X_2 \\ \partial x_2/\partial X_1 & \partial x_2/\partial X_2 \end{bmatrix}$$

$$\left\{ \begin{array}{c} \dot{F}_{11} \\ \dot{F}_{12} \\ \dot{F}_{21} \\ \dot{F}_{22} \end{array} \right\} = \left\{ \begin{array}{c} l_{11}F_{11} + l_{12}F_{21} \\ l_{11}F_{12} + l_{12}F_{22} \\ l_{21}F_{11} + l_{22}F_{21} \\ l_{21}F_{12} + l_{22}F_{22} \end{array} \right\}$$

$$\left\{ \begin{array}{c} \dot{x}_1 \\ \dot{x}_2 \\ \dot{F}_{11} \\ \dot{F}_{12} \\ \dot{F}_{21} \\ \dot{F}_{22} \end{array} \right\} = \left\{ \begin{array}{c} v_1 \\ v_2 \\ l_{11}F_{11} + l_{12}F_{21} \\ l_{11}F_{12} + l_{12}F_{22} \\ l_{21}F_{11} + l_{22}F_{21} \\ l_{21}F_{12} + l_{22}F_{22} \end{array} \right\}$$

system of ODEs with initial conditions

$$x_1 = X_1\,,\ x_2 = X_2\,,\ F(0) = I$$

This system can be integrated in time to get Lagrangian description of motion.

Strain magnitude

Lagrange strain $$E = \frac{1}{2}(F^T F - I)$$

Frobenius norm $$||E|| = \sqrt{E : E}$$

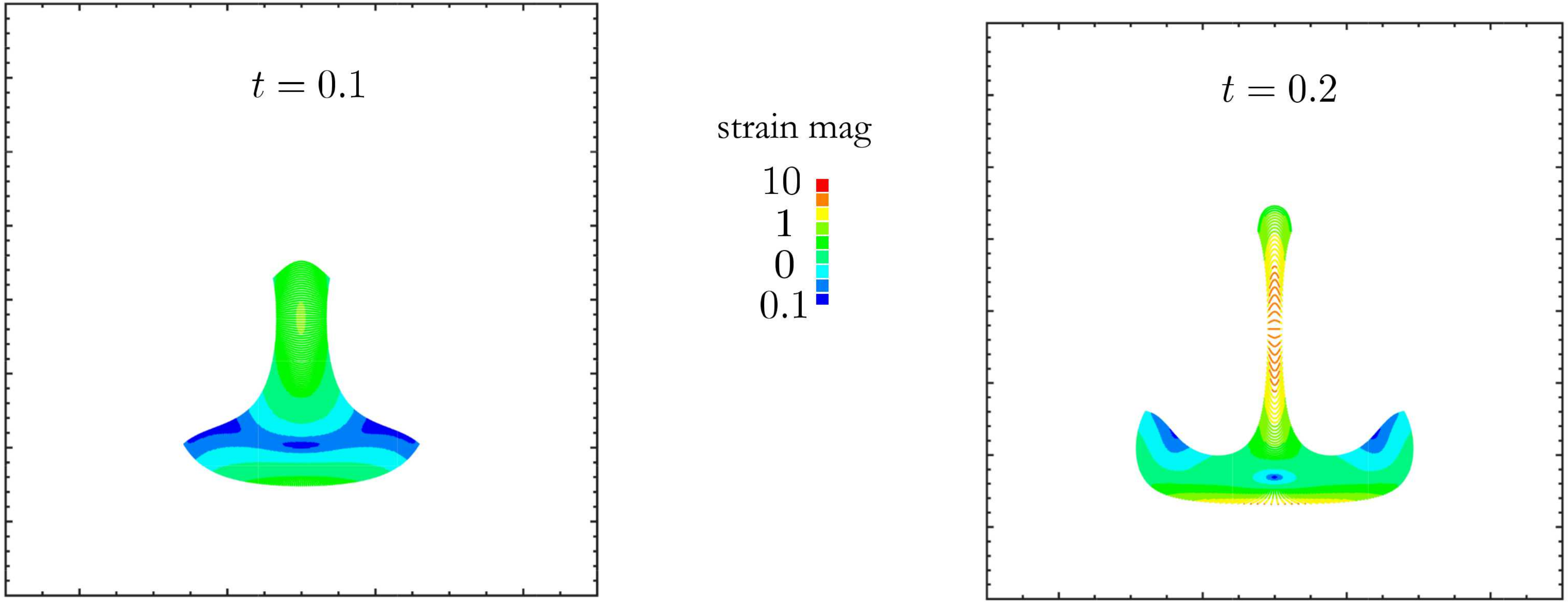

Compare best approximation in H^1: FE vs. MLS

- FE bilinear quad
- MLS: linear reproduction{1 x y}, support size = 2 dx
- look at effect of initial mesh distortion

Lagrangian motion (mesh interpolation)

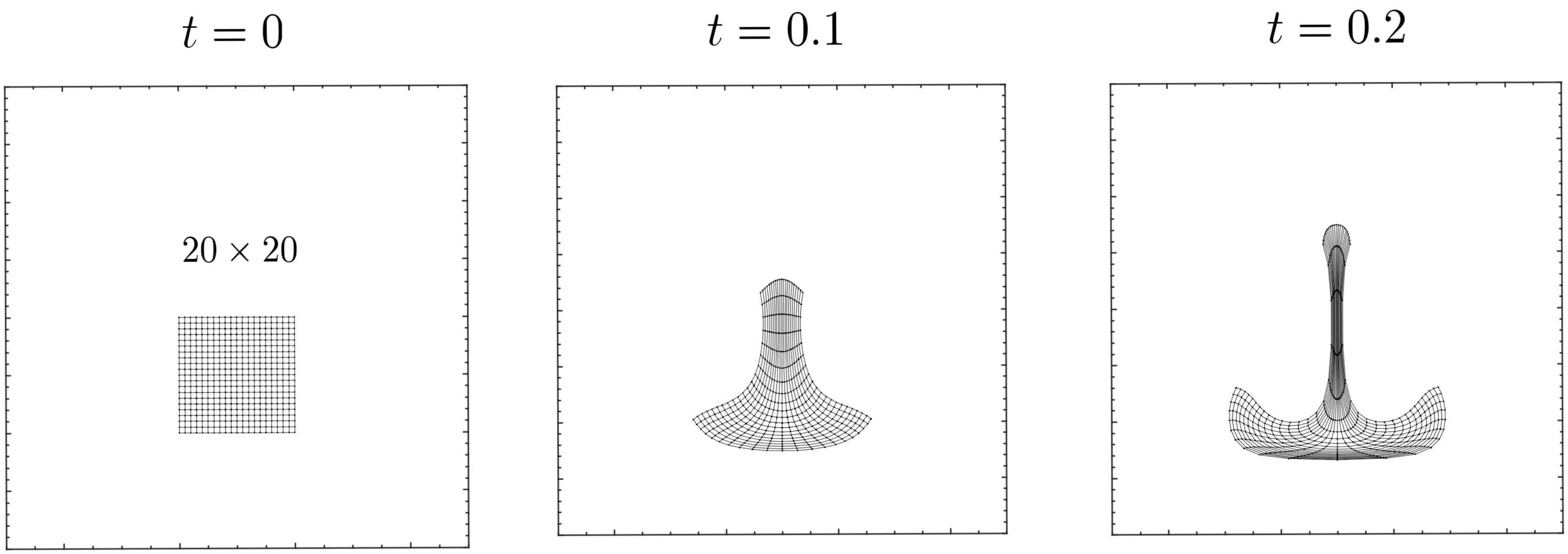

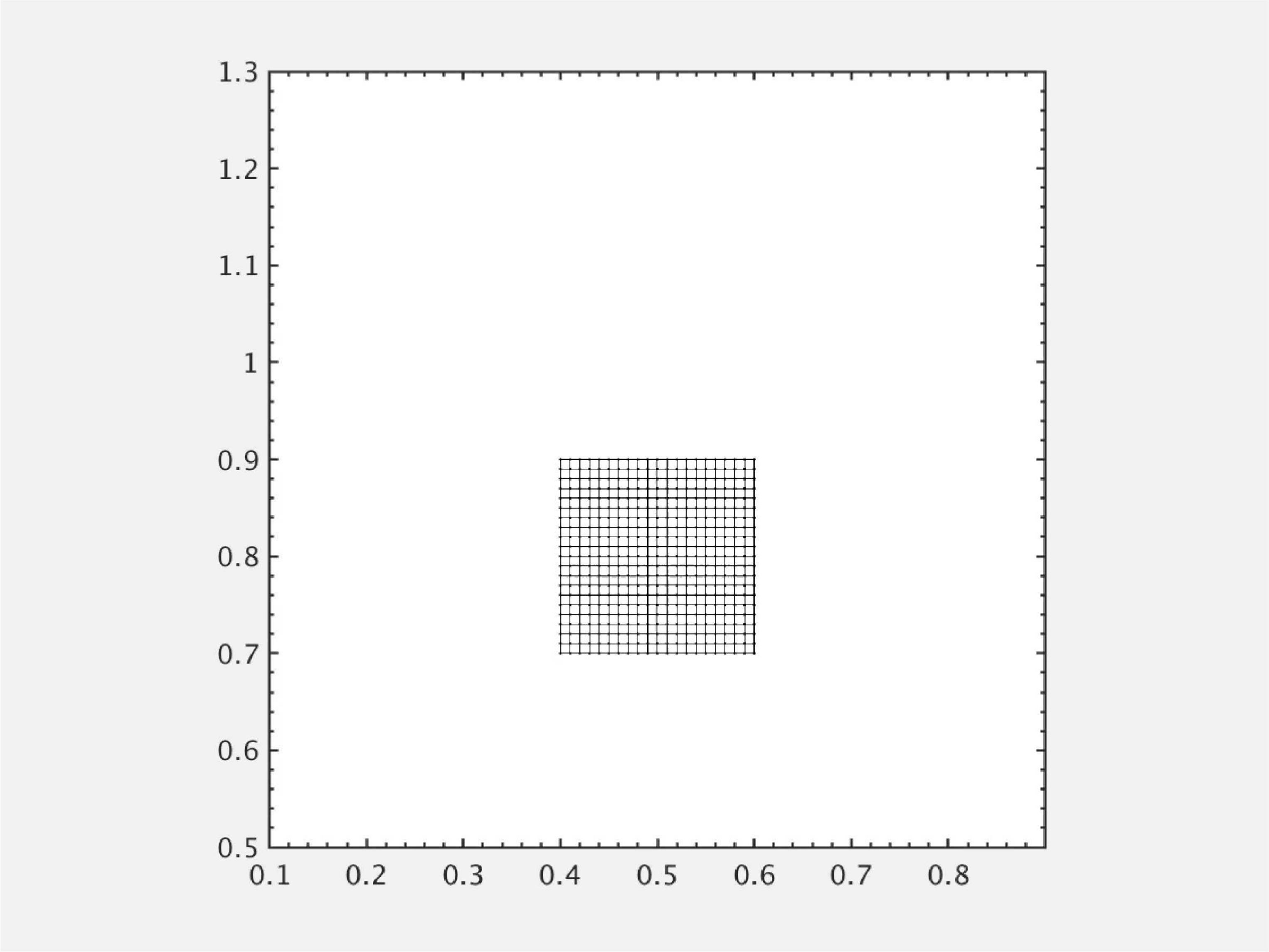
1.3
1.2
1.1
1
0.9
0.8
0.7
0.6
0.5
0.1
0.2
0.3
0.4
0.5
0.6
0.7
0.8

FE vs. meshfree (MLS)

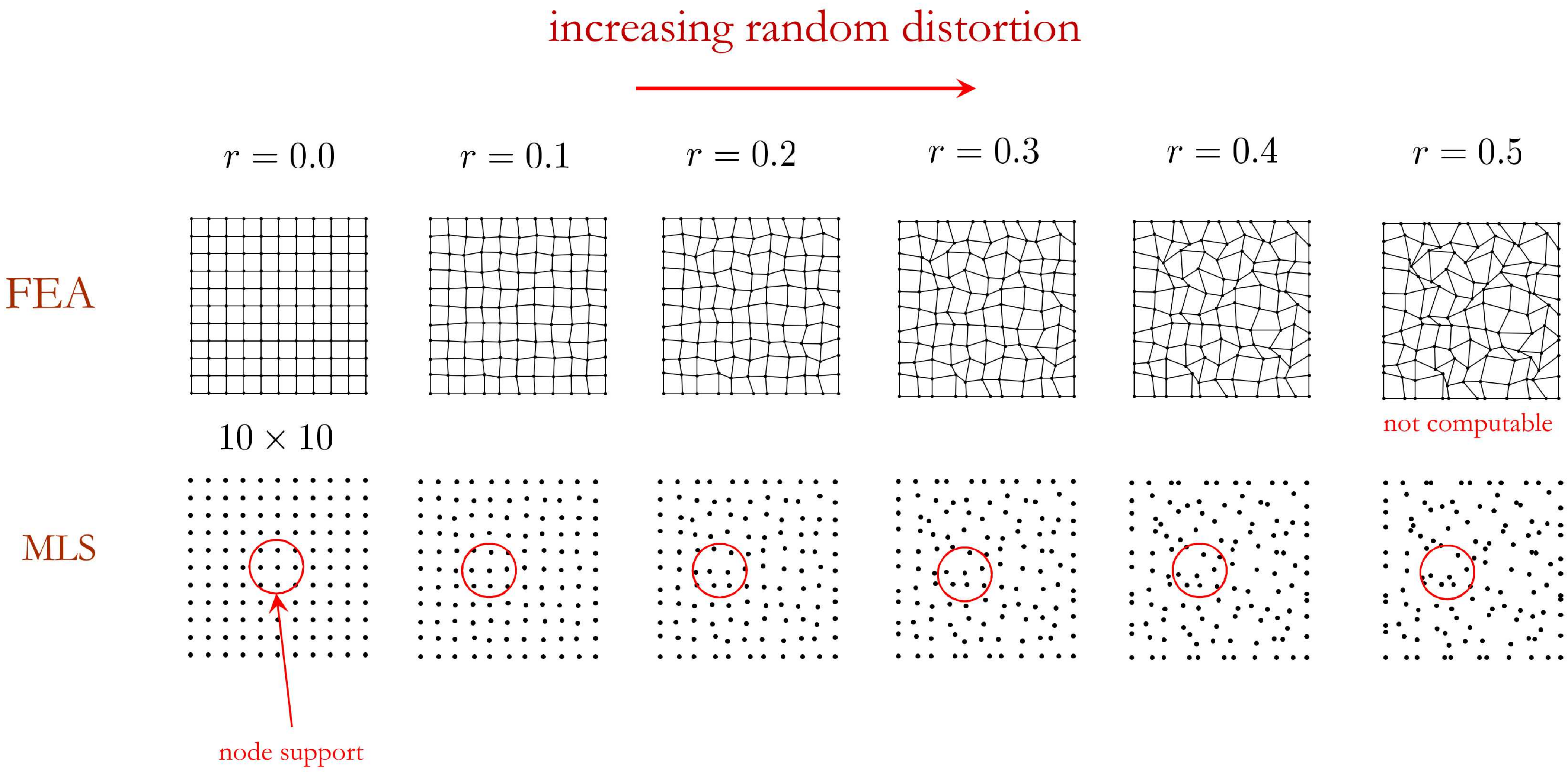

Best-approximation error comparison

L^2 convergence at a fixed time

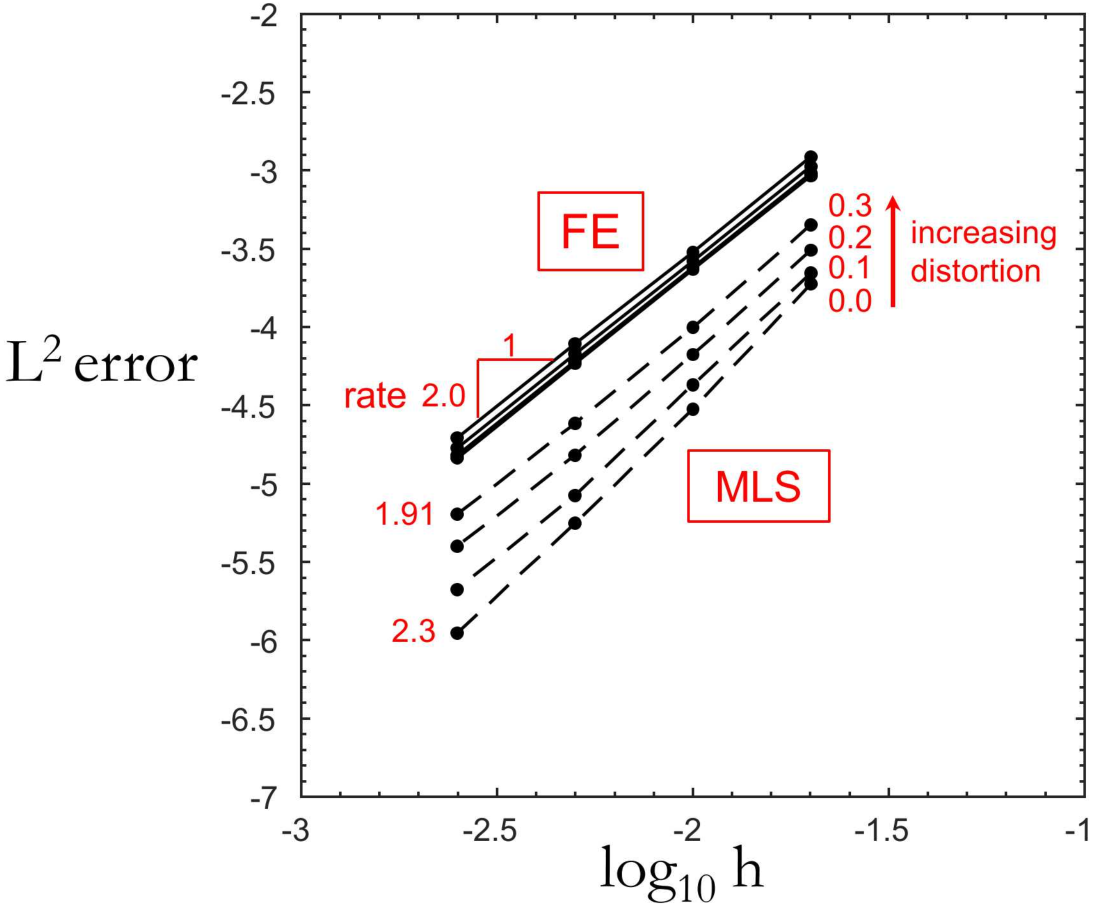

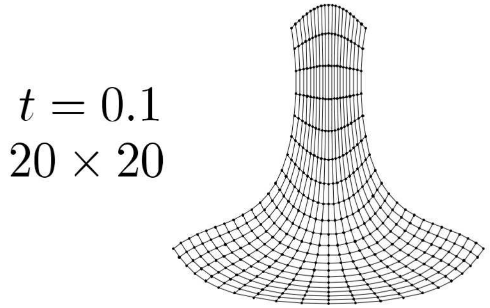

- MLS is significantly more accurate than FE.
- MLS error is sensitive to "distortion" compared to FE.

Best-approximation error comparison

H^1 convergence at a fixed time

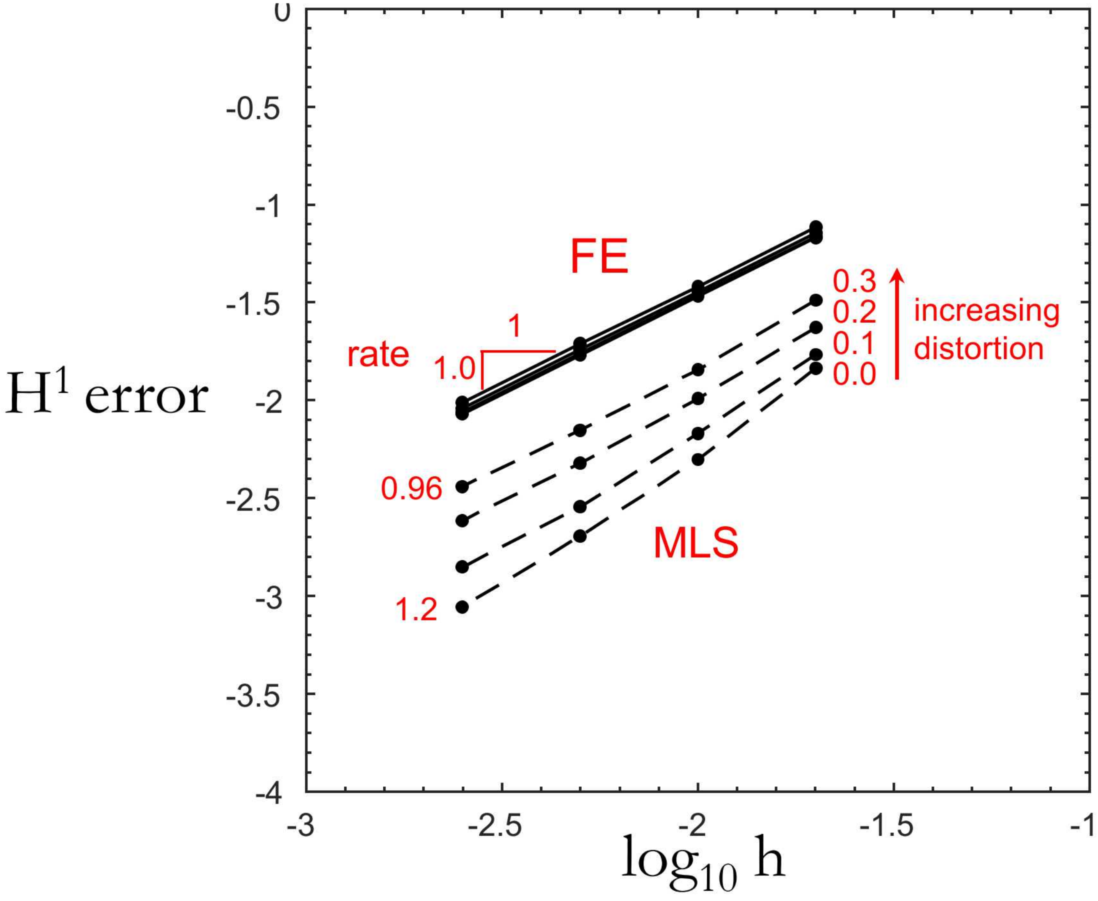

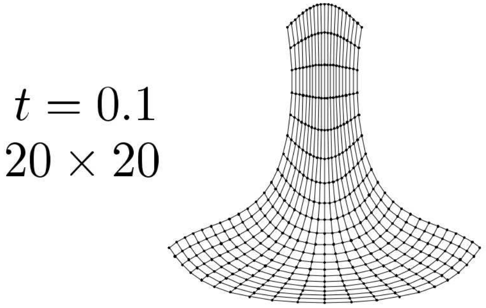

- MLS is significantly more accurate than FE.
- MLS error is sensitive to "distortion" compared to FE.

Robustness

H^1 error in time for a fixed mesh

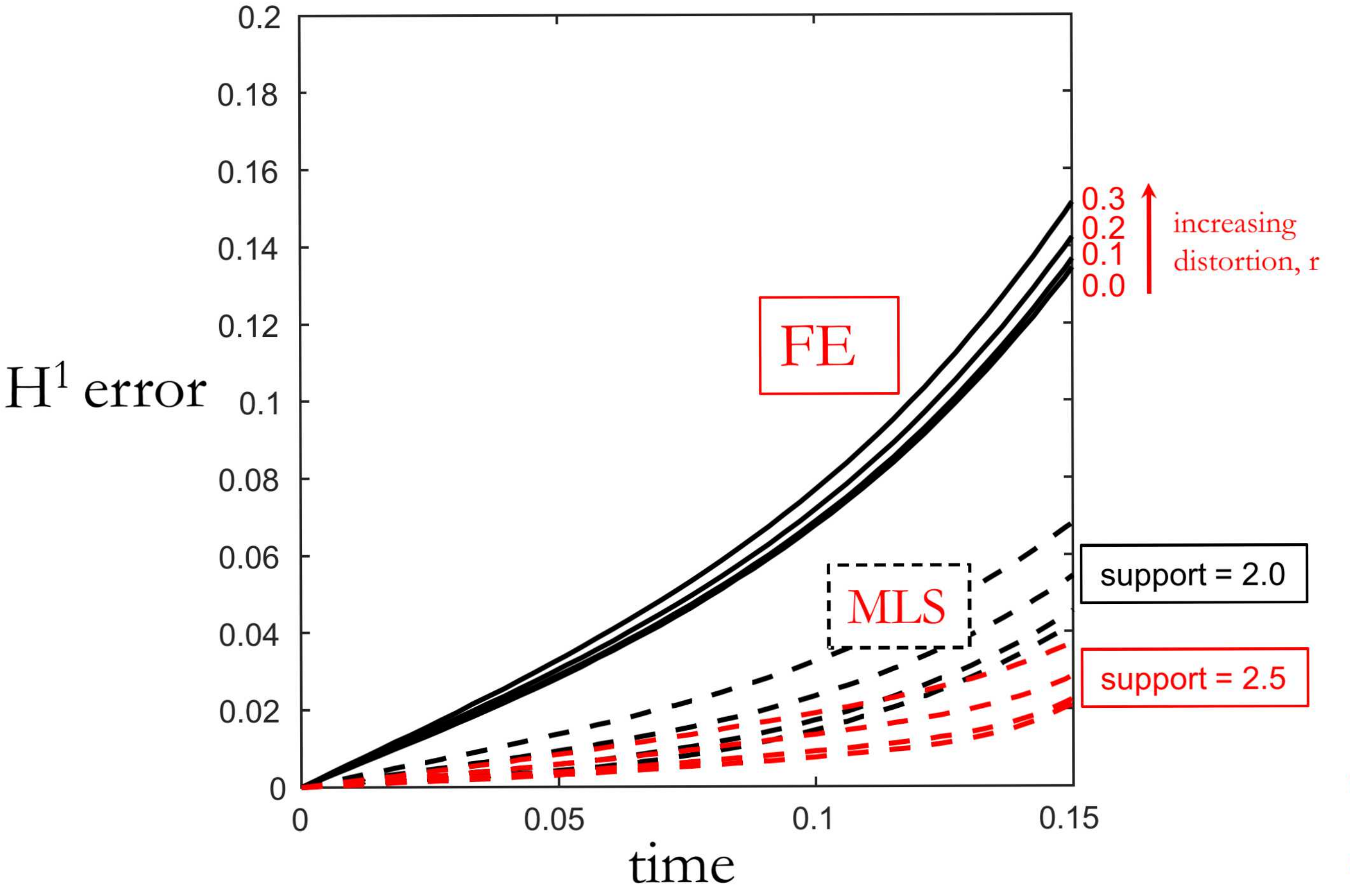

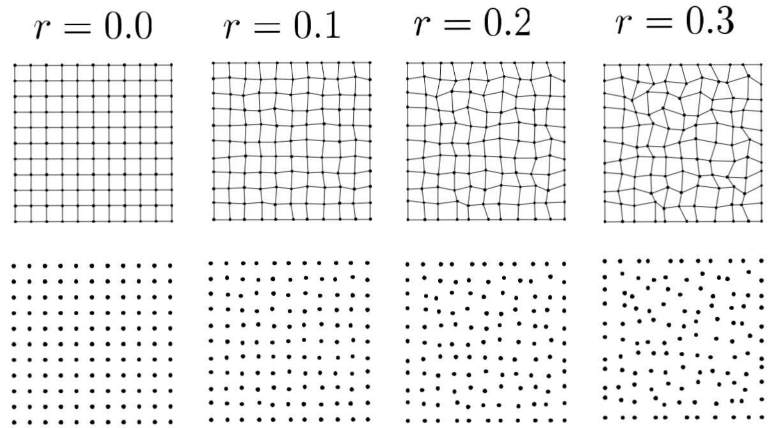

- MLS is significantly more accurate than FE.
- Increasing support size of MLS increases accuracy.

Summary

1. Examples of limitations of mesh-based discretizations for extreme events.
2. Developing manufactured solutions to compare robustness of FE vs. meshfree discretizations in large deformation regime.
3. Exploring best-approximation error in L^2 and H^1 norms.
4. Will also explore surface representations and adaptivity.